Eur Spine J (2001) 10 : 30–37
DOI 10.1007/s005860000211

ORIGINAL ARTICLE

C. Knop
U. Lange
L. Bastian
M. Oeser
M. Blauth

Biomechanical compression tests with a new implant for thoracolumbar vertebral body replacement

Received: 16 November 1999
Revised: 10 June 2000
Accepted: 11 August 2000
Published online: 22 November 2000

C. Knop (✉) · U. Lange · L. Bastian
M. Oeser
Department of Trauma Surgery,
Hannover Medical School,
30623 Hannover, Germany
e-mail: Dr.Christian.Knop@T-Online.de,
Tel.: +49-511-5322026,
Fax: +49-511-5325877

M. Blauth
Department of Trauma Surgery,
Ludwig-Franzens University,
Innsbruck, Austria

Abstract The authors present an investigation into the biomechanical functioning of a new titanium implant for vertebral body replacement (Synex). Possible indications are fractures and/or dislocations with damage of the anterior column, post-traumatic kyphosis and tumors of the thoracolumbar spine. The construction must be supplemented by a stabilizing posterior or anterior implant. For best fit and contact with adjacent end-plates, Synex is distractable in situ. We performed comparative compression tests with Synex and MOSS ("Harms mesh cage") on human cadaveric specimens of intact vertebrae (L1). The aim of the study was to measure the compressive strength of the vertebral body end-plate in uniaxial loading via both implants to exclude collapse of Synex in vivo. Twelve human cadaveric specimens of intact vertebrae (L1) were divided into two identical groups (matched pairs) according to bone mineral density (BMD), determined using dual-energy quantitative computed tomography (DE-QCT). The specimens were loaded with an axial compression force at a constant speed of 5 mm/min to failure, and the displacement was recorded with a continuous load-displacement curve. The mean ultimate compression force (F_{max}) showed a tendency towards a higher reading for Synex: 3396 N versus 2719 N (non-significant). The displacement until F_{max} was 2.9 mm in the Synex group, which was half as far as in the MOSS group (5.8 mm). The difference was significant ($P<0.001$). The compression force was twice as high, and significantly ($P<0.05$) higher with Synex at displacements of 1 mm, 1.5 mm and 2 mm. A significant ($P<0.001$) correlation ($R=0.89$) between F_{max} and BMD was found. Synex was found to be at least comparable to MOSS concerning the compressive performance at the vertebral end-plate. A possible consequence of the significantly higher mean compression forces between 1 and 2 mm displacement might be decreased collapse of the implant into the vertebral body in vivo.

Keywords Thoracolumbar spine · Vertebral body replacement · Implant · Compression · Biomechanics · Bone mineral density · Synex · MOSS · Harms mesh cage

Introduction

Various operative techniques are described for restoration of form and function of the thoracolumbar spine for patients with unstable traumatic lesions, tumors, or post-traumatic deformity [1,2 3, 7, 8, 9, 10, 11, 13, 20, 21, 25, 27, 28, 29, 34, 35, 36, 39, 40]. The standard procedure most commonly practised these days is posterior stabilization with an angularly stable internal fixation device [4, 5, 6, 22, 24].

A *combined posterior-anterior approach* should allow immediate weight-bearing of the anterior spine and reliable fusion with no loss of correction [5, 6, 7, 11, 13, 20]. However, this approach has its own drawbacks: on the one hand we have observed increased morbidity as a result of harvesting strut grafts from the iliac crest while, on the other, complications specific to the procedure itself have occurred, e.g. healing problems or graft fracture. There are still no long-term results confirming the superiority of this method and justifying the extra effort involved [4, 6, 23].

Synex (STRATEC Medical, Oberdorf, Switzerland) is a new titanium implant for vertebral body replacement designed to avoid the disadvantages of bone removal from the iliac crest and, at the same time, restore normal load-bearing in the anterior spine and normal load-sharing between anterior and posterior column of the spine (Fig. 1 A). The range of indications for the implant include traumatic lesions, post-traumatic kyphosis, tumors, and infections of the thoracolumbar spine. Synex is a hollow titanium implant that can be distracted in situ after interbody placement in the spinal lesion, with a view to ensuring a permanently secure fit with axial loadability and minimizing the risk of secondary dislocation and loss of correction. The operation itself is made easier by the fact that the implant is smaller than the anterior defect when first fitted, and is only distracted to the desired height with a special distractor after precise positioning (Fig. 1 B). Our own clinical experience with MOSS (DePuy Orthopädie GmbH, a Johnson&Johnson Company, Sulzbach, Germany) has shown that the placement may be problematic. A subsequent operation as a third step for the tensioning of posterior fixation was recommended [34, 35].

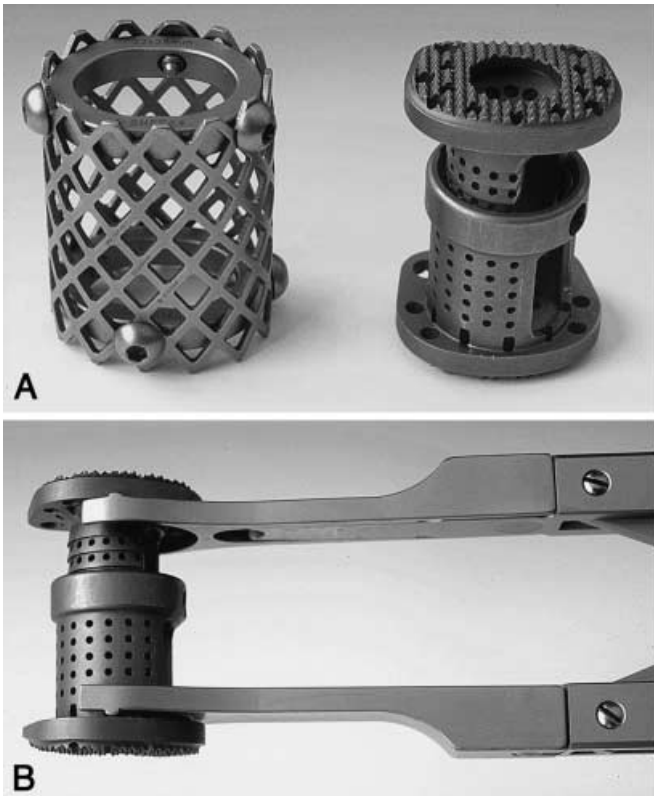

Fig. 1A, B Synex and MOSS. **A** Original implants, **B** Synex in the distractor

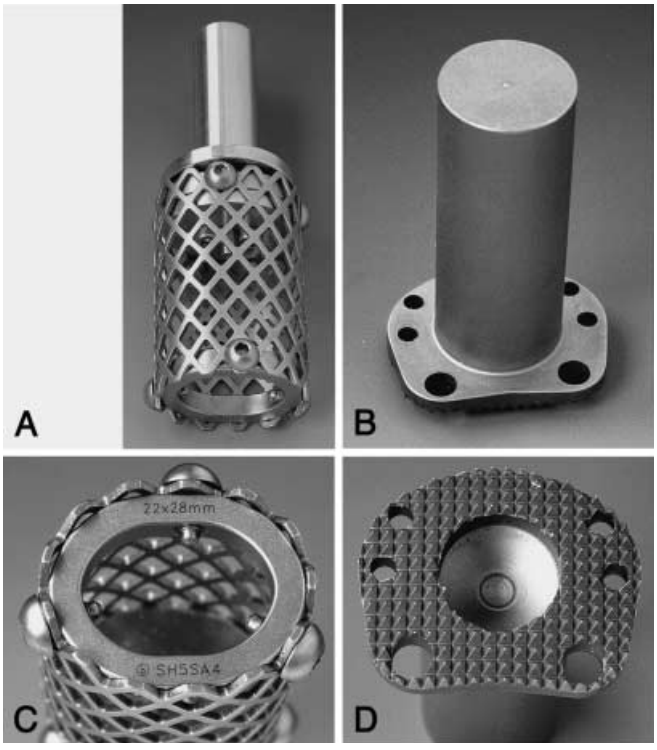

Fig. 2A–D Test implants. **A** MOSS with attached punch for fixation in the test machine, **B** Synex test punch, **C** top view of MOSS with inserted internal stabilization ring, and **D** top view of Synex test punch

We performed comparative biomechanical tests to investigate the compressive performance of implants in the vertebral bodies. For comparison purposes we tested the corresponding size of the MOSS vertebral body replacement spacer ("Harms mesh cage") fitted with an internal stabilization ring, as this implant has already been in use for several years (Fig. 2). This compression testing at constant speed should quantify, firstly, the displacement of both implants as they "settle," i.e., sink into the end-plates of the vertebral body and, secondly, the compression forces transmitted at the interface between implant and vertebral body. With this test series we wanted to determine whether the end-plates of the newly developed implant were at least as suitable as those of the MOSS spacer for transmitting compression forces or whether rapid collapse is likely to occur.

Materials and methods

We used exclusively freshly collected human vertebral body specimens of L1 with no macroscopically visible pathological or severe degenerative changes. After removal, the vertebral bodies were freed of adjoining tissue, sealed in plastic bags and frozen to –18°C. The cortical and cancellous bone mineral densities (BMD_{cort} and BMD_{canc}) of the specimens were determined in a water-bath by dual-energy quantitative computed tomography (DE-QCT; Somatom plus S, Siemens, Munich-Erlangen, Germany), using OsteoCT software and a reference phantom [12, 15, 17, 19, 26, 31, 32, 33]. The end-plates of the individual vertebral bodies were embedded in hard plaster for the trials, and the vertebral body end-plates were aligned as horizontally as possible (Fig. 3). This solid hard plaster bed was placed on the horizontal baseplate of the test device. Slight movements of the vertebral bodies were excluded by plaster embedding with a horizontal cutoff at the base.

The test conditions formulated by Wilke et al. [37] were observed during handling of the specimens in the preparatory and test phases. Twelve specimens of L1 vertebral bodies were assigned to two comparable groups of six vertebrae, matched for age of death and bone mineral density (matched pairs). The specimens in group M were tested with MOSS, those of group S with Synex.

We tested the following two implants:

- MOSS vertebral body replacement ("Harms mesh cage") size 3 with an oval cross-section of 22×28 mm. The implant was fitted, at the "test end", with the original internal stabilization ring, which was secured inside the cage with three screws. The ring was deliberately not fitted flush with the edge of the cage, but was countersunk by 2 mm, as described for the use in vivo [34]. The opposite end ("machine end") of the cage was equipped with a steel punch specially produced for these tests. The punch was connected to the titanium cage, without twisting, via a second original internal stabilization ring. The vertical compression force was applied to the upper end of the cage via the plate on this punch (Fig. 2).
- Synex vertebral body replacement. For the tests we used a solid titanium punch specially produced for the tests, whose "test end" was constructed to match that of the end-plate of the original implant, with an oval cross-section of 25×28 mm. We selected this type of test implant since it would not have been possible to clamp an original Synex in the test device (Fig. 2).

Fig. 3 Vertebral body specimen embedded in hard plaster

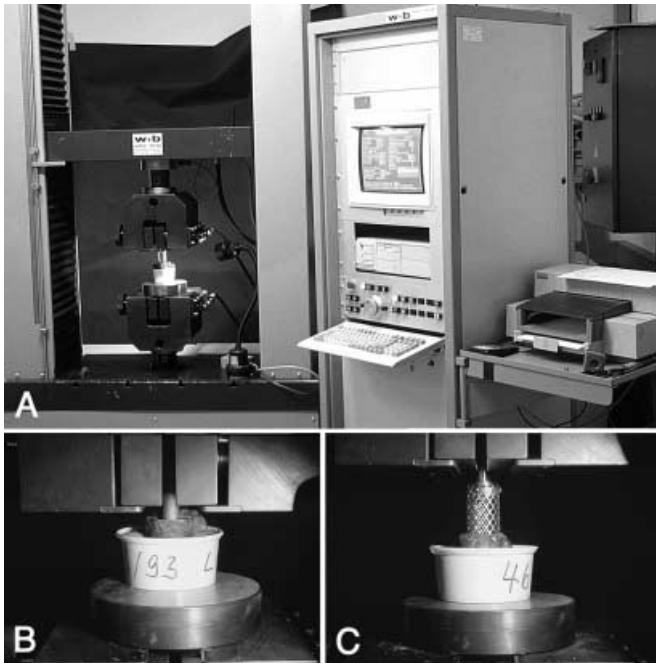

Fig. 4 **A** Overview of the universal test machine. **B, C** Detail view of the electromechanical test unit with specimen and mounted Synex (**B**) and MOSS (**C**) implant

We conducted these tests at the Institute for Materials Testing, Hannover Technical University. The solid rods at the "machine end" of both test implants were clamped in the hydraulic chucks of the universal test machine [100 kN universal test machine (electromechanical); Walter+Bai Company, Löhningen, Switzerland, type LFEM 100/1400, serial no. 339 with hydraulic chucks; control panel with digital measuring and control electronics, model PCS-200, no. 68 with provision for hydraulically-operated chucks; semi-automated extension sensor MFN-A500/2; class 1 force measurement accuracy according to DIN 51220–23, relative read-out error q<0.21% (specification: q<0.5%); calibration certificate F001400 dated 09.06.98], so as to position them in vertical alignment above the "test end". The vertebral body was placed on the horizontal baseplate of the test machine in a horizontal and fixed position in relation to the axial direction of the compression force (Fig. 4). The specimen was positioned such that the implant was aligned with the center of the end-plate in the sagittal and frontal planes. The center of the end-plate was defined as half way along the sagittal and transverse diameter of the vertebral body. The position was only checked by sight, following the implantation in vivo. The movable hydraulic head of the test machine, with the implant clamped in position, was manually lowered until the implant made contact with the upper end-plate (compression force of F_0<10 N). This position was the starting point (distance d_0) of every test. The machine was switched on and the hydraulic head with fitted implant moved vertically downward at a constant speed of v=5 mm/min. The electronic measuring unit of the test machine plotted the distance d travelled by the hydraulic head plus implant and the compression force F, determined by the electronic sensor incorporated in the head, as a continuous load-displacement curve. Every test ended when the end-plate of the specimen had completely and very perceptibly caved in, with a resulting clear drop in force.

Table 1 Data for specimens and results measured in the tests with Synex (group S)

	Age (years)	BMD_{canc} (mg/cm³)	BMD_{cort} (mg/cm³)	d_{max} (mm)	F_0 (*N*)	$F_{0.5\,mm}$ (*N*)	$F_{1.0\,mm}$ (*N*)	$F_{1.5\,mm}$ (*N*)	$F_{2.0\,mm}$ (*N*)	F_{max} (*N*)
N	6	6	6	6	6	6	6	6	6	6
Mean	41.7	117.7	261.4	2.9	4.2	240.7	861.8	1806.2	2605.2	3395.5
Median	41.0	130.5	274.9	2.9	3.3	230.5	809.0	1767.0	2460.5	3096.0
SD	10.5	47.1	65.3	0.5	3.1	159.3	428.6	946.5	1206.8	1312.0
Min	31.0	42.9	146.8	2.1	0.7	30.0	342.0	854.0	1416.0	2109.0
Max	55.0	167.4	323.0	3.5	8.0	502.0	1588.0	3421.0	4648.0	5446.0
P-*value*[a]	∅	∅	∅	<0.001	∅	∅	0.037	0.024	0.01	∅

[a] Significance of difference with the comparator group (*t*-test)

Table 2 Data for specimens and results measured in the tests with MOSS (Group M

	Age (years)	BMD_{canc} (mg/cm³)	BMD_{cort} (mg/cm³)	s_{max} (mm)	F_0 (*N*)	$F_{0.5\,mm}$ (*N*)	$F_{1.0\,mm}$ (*N*)	$F_{1.5\,mm}$ (*N*)	$F_{2.0\,mm}$ (*N*)	F_{max} (*N*)
N	6	6	6	6	6	6	6	6	6	6
Mean	43.3	112.8	274.8	5.8	4.2	211.0	399.0	714.2	925.0	2719.2
Median	47.0	114.0	291.0	6.1	3.7	223.0	400.0	584.5	752.5	2453.0
SD	15.5	44.3	85.8	0.9	2.4	109.1	198.8	346.1	445.9	1466.3
Min	23.0	46.3	137.8	4.4	2.0	48.0	175.0	430.0	491.0	826.0
Max	60.0	164.4	379.6	6.9	8.0	336.0	682.0	1310.0	1638.0	4741.0
P-value[a]	∅	∅	∅	<0.001	∅	∅	0.037	0.024	0.01	∅

[a] Significance of difference with the comparator group (*t*-test)

The values determined for distance *d* travelled and force *F* were tested for normal distribution by the Kolmogorov-Smirnov method with significance correction according to Lilliefors: since normal distribution was assumed, we were able to compare for statistically significant differences between the two groups using the *t*-test.

Results

The two test groups showed no significant differences as regards age of the donor or BMD of the L1 specimens used, and could thus be considered as equivalent (Table 1, Table 2). In the S group (Synex) we used vertebral bodies from one female and five male donors with a mean age of 41.7 (range 31–55) years. The average mineral density of cancellous bone, BMD_{canc}, was 117.7 mg/cm³ (range 42.9–167.4 mg/cm³), while that of cortical bone, BMD_{cort}, was 261.4 mg/cm³ (range 146.8–323.0 mg/cm³). In the M group (MOSS) the specimens originated from 4 male and 2 female cadavers with an average age of 43.3 (range 23–60) years. The mean BMD values were 112.8 mg/cm³ (range 46.3–164.4 mg/cm³) for BMD_{canc} and 274.8 mg/cm³ (range 137.8–379.6 mg/cm³) for BMD_{cort}.

The force F_0 determined at the starting point d_0 of every test was identical in the two groups: F_0=4.2 N(range 0.7–8.0 N) in group S and F_0=4.2 N (range 2.0–8.0 N) in group M. In both groups the compression force was increased after the start of the test, whereupon the implants "settled" onto the end-plate of the specimens. This was followed by a period of force increase until, finally, the vertebral body end-plate caved in and the force dropped (Fig. 5).

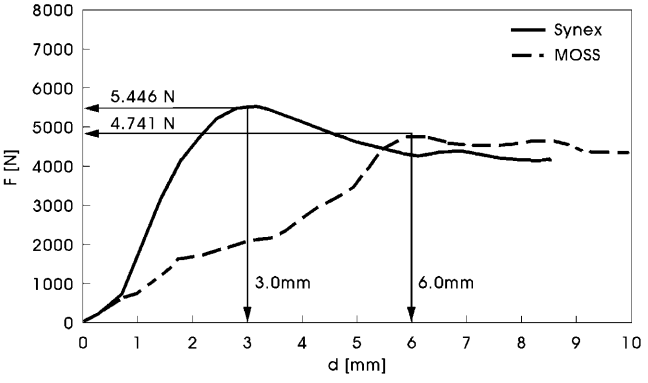

Fig. 5 Load-displacement curves of the two specimens with highest bone mineral density (BMD) in each group. The cancellous BMD (BMD_{canc}), mean ultimate compression force (F_{max}) and mean maximum displacement (d_{max}) for the two groups were: *group S* BMD_{canc}=167 mg/cm³, F_{max}=5446 N, d_{max}=3.0 mm; *group M* BMD_{canc}=164 mg/ cm³, F_{max}=4741 N; d_{max}=6.0 mm

The mean distance travelled, d_{max}, until the onset of maximum compression force, F_{max}, in the S group, was 2.87 mm (range 2.10–3.53 mm), which was half the mean distance of 5.83 mm (range 4.40–6.86 mm) covered in the M group. This difference was significant (P<0.001). The force F_0 was identical in both groups at the start of the

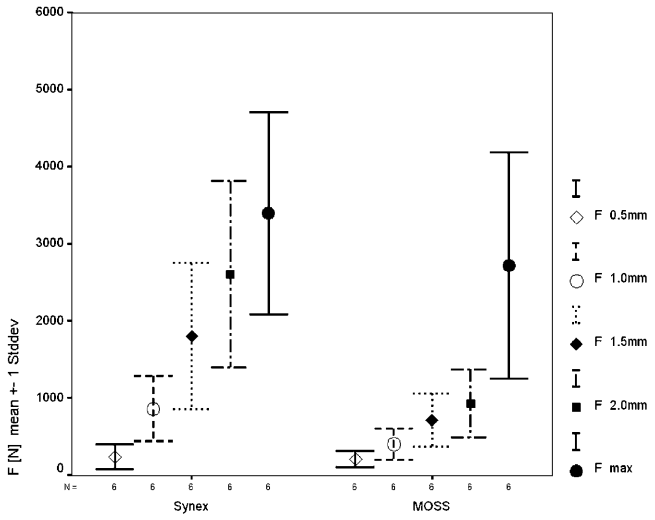

Fig. 6 Grouped error bar chart showing mean values ±1 standard deviation (SD) for compression force F at 0.5–2.0 mm and the maximum compression force F_{max}

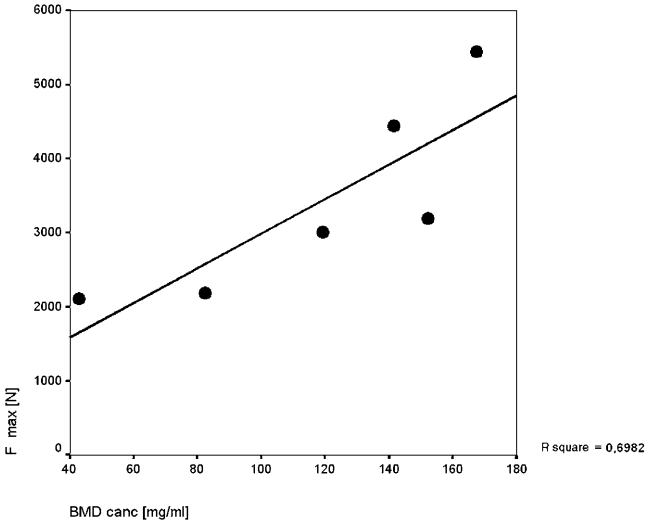

Fig. 7 Regression lines showing the significant correlation between the maximum compression force F_{max} and trabecular bone mineral density, BMD_{canc}, in group S. The correlation coefficient R^2 was 0.6982

measurement (d_0). While the difference was not statistically significant after a distance travelled, d ,of 0.5 mm, a trend towards a higher force was apparent in the S group ($F_{0.5mmS}$=241 N vs $F_{0.5mmM}$=211 N; P=0.81). The difference in the compression forces F determined thereafter increased with distance travelled and, after distances of 1.0–2.0 mm, the average force was over twice as high in the S group (Table 1, Table 2, Fig. 6). The differences were significant for d=1.0 mm (P=0.037), d=1.5 mm (P=0.024) and d=2.0 mm (P=0.01). The average maximum force F_{max} after a distance of d_{max} tended to be higher in the S group (F_{maxS}=3396 N vs F_{maxM}=2719 N), though the difference failed to reach the level of statistical significance (P=0.419).

There was a statistically significant linear correlation in both groups between the maximum compression force F_{max} and cancellous bone mineral density, BMD_{canc}, of the respective vertebral body (Fig. 7, Fig. 8). In the S group, the correlation coefficient according to Pearson was R_S=0.836 (P=0.038) and, in the M group c_M=0.982 (P=0.001). The following regression equations were determined for the assumption of this linear correlation:

$$F_{max\,(Synex)} = 23.3 \cdot BMD_{canc} + 654$$

$$F_{max\,(MOSS)} = 32.5 \cdot BMD_{canc} - 946$$

As an approximate value we calculated a theoretical "standard compression force" F_{stand}, based on a "standard BMD" of 100 mg/cm^3 as a quotient of compressive force and BMD, multiplied by a factor of 100:

$$F_{stand} = \frac{F}{BMD_{canc}} \cdot 100$$

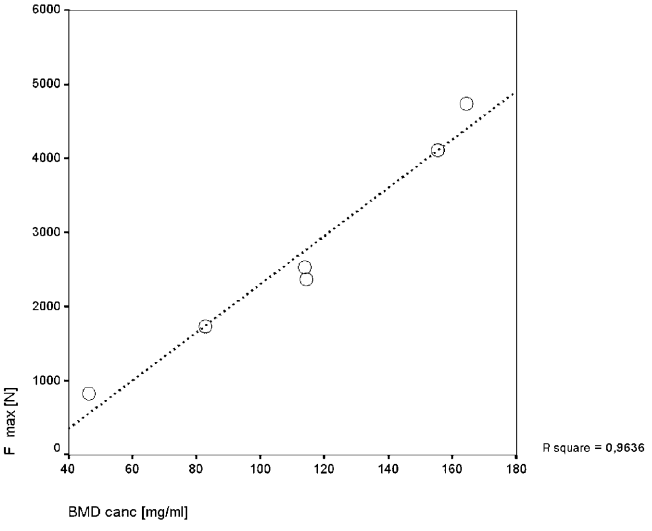

Fig. 8 Regression lines showing the significant correlation between the maximum compression force F_{max} and trabecular bone mineral density BMD_{canc} in group M. The correlation coefficient R^2 was 0.9636

Comparing this approximate figure, we also determined significant differences, with a higher force in the S group in each case for the force F_{stand} at 1.0 mm, 1.5 mm and 2.0 mm (Table 3). The "standardized" maximum force in the S group, F_{stand} (max), was 3094 N, which was much higher than the equivalent value of 2285 N for the M group, though the difference just failed to reach the level of statistical significance (P=0.093).

Table 3 Theoretical compression forces F_{stand} (N) with Synex (group S) and MOSS (group M), calculated according to a standardized bone density BMD_{canc}=100 mg/cm³ according to:

$$F_{stand} = \frac{F}{BMD_{canc}} \cdot 100$$

[a] Significance of difference with the comparator group (*t*-test)

	$F_{stand\ 0.5\ mm}$		$F_{stand\ 1.0\ mm}$		$F_{stand\ 1.5\ mm}$		$F_{stand\ 2.0\ mm}$		$F_{stand\ max}$	
	S	M	S	M	S	M	S	M	S	M
Mean	185.4	211.8	739.5	369.4	1585.2	674.8	2355.7	854.3	3094.2	2285.2
Median	194.7	225.3	739.3	400.1	1693.7	746.7	2411.0	888.1	2892.9	2160.1
SD	78.3	108.2	175.3	125.9	515.1	238.0	812.8	266.2	987.5	406.2
Min	69.9	30.9	490.8	123.6	752.1	279.9	1185.9	406.7	2096.6	1784.0
Max	299.9	358.5	948.6	479.3	2043.6	928.7	3531.5	1129.3	4916.1	2883.8
P-value	∅		0.002		0.006		0.002		∅ (0.093)	

Discussion

General test conditions and guidelines for the treatment of human vertebral body specimens have been formulated by Wilke et al. [37]. These were taken into account and observed during the tests.

Before we conducted the tests, the BMD values of all specimens were determined by DE-QCT, currently considered to be the method of choice [12, 15, 17, 19, 26, 31, 32, 33]. However, since the results of series investigations into BMD have shown considerable dispersion, only a range of physiological reference values exist. Reference values of 93–145 mg/cm³ have been reported for trabecular bone density for the age range of 20–59 years [12]. Ito et al. [17] determined values of 95.3–112.2 mg/cm³ for trabecular BMD and 228.8–379.0 mg/cm³ for cortical BMD. But these figures were only comparable to a limited extent, since we anticipated a systematic difference when determining bone density of isolated vertebral bodies in a water bath. In our test series the standardized measurement of BMD was crucial in ensuring identical preconditions in both test groups. The bone densities determined for our specimens were comparable to the in vivo figures.

The literature offers no uniform recommendations for the test conditions in compression trials of this type, and test speeds of 5 mm/min [14, 30], 0.4 mm/s [18], 35 mm/min [38] and 2.54 mm/s [16] are described in the literature. Since no group of authors offers any rationale for their respective test speed, we assumed that the various speeds were determined by the test machine employed in each case. We selected a constant speed of 5 mm/min, a fairly slow test speed that should ensure improved observation of any changes at the interface between implant and vertebral body. A current test certificate confirmed that the test machine used met all the official quality criteria. Additionally, the test series was professionally supervised at the Materials Testing Laboratory of the Hannover Technical University.

All 12 tests proceeded as expected. Since no irregularities in the load-displacement curve and no positional changes of the specimens or changes in the plaster embedding were observed, all 12 tests could be evaluated.

In both tested implants – and as expected – a steady rise in compression force during the first few millimeters of the test run resulted in a "settling" of the prominent ends of the implant in the end-plate of the vertebral body. During testing of the Synex implant, this proved to be a significantly shorter distance, even with a sharp rise in force, thanks to the surface arrangement of 1-mm-high tips whose cross-sections increase towards the implant surface. The MOSS implant sank into the end-plate with a flatter rise in compression force until the internal stabilization ring, countersunk to a depth of 2 mm, checked up against the end-plate, whereupon the force increased more sharply. The maximum compression force F_{max} measured for the MOSS implant was reached only after it had covered double the distance, requiring an average of 5.8 mm of collapse into the vertebral body end-plate until the point of maximum resistance, compared to an average distance of 2.9 mm for the Synex. This 2.9-mm discrepancy could represent a small additional loss of correction when using the MOSS implant compared with Synex.

A margin of less then 2 mm would lead to earlier contact between the stabilizing ring and the end-plate, likely resulting in less displacement and higher compressive forces with MOSS. The use of the Harms cage in vivo was also described without the inner stabilizing ring [34], under which conditions one would expect a decreased maximum compressive force and greater settling of the implant into the vertebral body.

Comparing the mean maximum compressive forces of both implants, we demonstrated a difference of 20% favoring Synex (Synex 3396 N, MOSS 2719 N), which was not significant. Comparison of the contact areas of the two implants (Fig. 2) revealed a difference of 16% favoring Synex (Synex 360 mm², MOSS 302 mm²). Due to the higher difference in the mean maximum compressive forces, we also calculated a higher mean maximum point loading, which was revealed to be 9.4 N/mm² for Synex and 9.0 N/mm² for MOSS. Although these differences may indicate a better compressive performance with Synex, the differences were not significant.

The following average maximum compression forces were measured with various grafts or implants against the vertebral body end-plate by Hollowell et al. [16]: 1473 N ("Harms mesh cage", 17×22 mm), 1165 N (iliac crest bone graft), 1038 N (humerus), 1037 N (3×ribs) and 537 N (1×rib). The deformation (distance covered) measured for

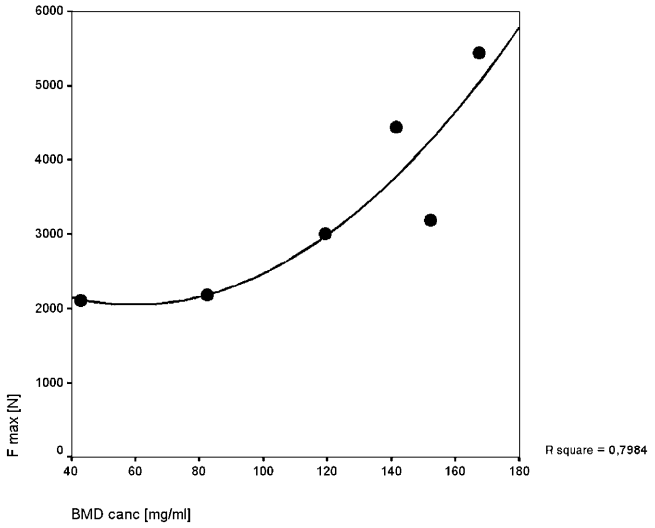

Fig. 9 Curve adjustment for exponential regression between the maximum compression force F_{max} and trabecular bone mineral density BMD_{canc} in group S. The correlation coefficient R^2 was 0.7984

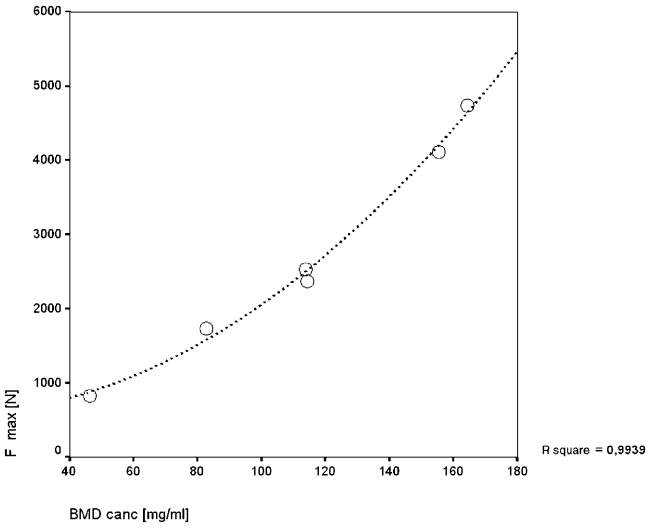

Fig. 10 Curve adjustment for exponential regression between the maximum compression force F_{max} and trabecular bone mineral density BMD_{canc} in group M. The correlation coefficient R^2 was 0.9939

the "Harms mesh cage" was 5.9 mm, i.e., almost identical to our own results.

Hollowell et al. [16] also mentioned a statistically significant correlation (P<0.001) between BMD and maximum compression force, though they do not provide any figures to demonstrate the statistical quality of this correlation. Hansson et al. [14] found a linear correlation between BMD and maximum compression force, calculating a significant (P<0.01) correlation coefficient of 0.81–0.90. In compression tests with "interbody cages" between vertebral bodies, Jost et al. [18] observed a significant (P<0.0005) linear correlation between the above variables.

We calculated regression equations for Synex and MOSS for the significant linear correlations observed between the cancellous bone mineral density and the maximum compression force. The constant determined in these calculations for MOSS was a negative figure (–946), which demonstrates the unreliability of the linear correlation since, in practice, one would only expect a force with a positive figure with a spongious bone mineral density set at 0. Curve adjustments for an exponential (non-linear) regression likewise showed good correspondence on the graph, with a significant (P_{Synex}=0.019; P_{MOSS}=0.0001) correlation (Fig. 9, Fig. 10), suggesting that an exponential correlation might also be possible. Tests with larger sample sizes would be needed for a more accurate analysis of the statistical relationship.

Although no data are currently available on the specific compression forces that are actually generated in the intervertebral space in vivo, clinical experience has shown that iliac crest bone grafts or MOSS perform their function between stabilized segments without any extreme loss of correction. The question regarding the proportion of the load borne by the vertebral body replacement or graft and the degree of the relieving effect provided by anterior or posterior implants remains unanswered. Many other factors with a potential influence on the therapeutic outcome are involved; for example, the surgical technique and the success of any intervertebral fusion. The results presented here, therefore, demonstrate only a theoretical advantage in favor of Synex, the significance of which needs to be assessed in further biomechanical tests with a three-dimensional spinal loading simulator or in clinical trials.

Conclusions

1. In comparison we observed significantly higher compressive forces with Synex™ with an average 2.9 mm less bony collapse on compression because of the 2 mm rim of the MOSS cage above the stabilization ring compared with the 1 mm height of the milling on the surface of the Synex implant. This might lead to slight reduction in postoperative settlement into kyphosis when the Synex implant is used.
2. We determined a strong correlation between trabecular BMD and the maximum compressive forces. A QCT scan in addition to the standard preoperative CT scan might be a helpful tool in detecting patients with a higher risk of postoperative implant failure.

Acknowledgements The authors would like to thank Stratec Medical, Oberdorf, Switzerland, for providing funding for this project; Mr R. Witte (grad. eng.) and Mr K. Oelker, Institute for Materials Testing, Hannover Technical University, for the professional supervision of the test series; and Dr. M. Török, Department of Biomathematics and Biometrics, Hannover Medical School, for checking the statistical analysis.

References

1. Aebi M, Etter C, Kehl T, Thalgott J (1988) The internal skeletal fixation system. A new treatment of thoracolumbar fractures and other spinal disorders. Clin Orthop 227:30–43
2. Bayley JC, Yuan HA, Fredrickson BE (1991) The Syracuse I-plate. Spine 16 [3 Suppl]:120-124
3. Been HD (1991) Anterior decompression and stabilization of thoracolumbar burst fractures by the use of the Slot-Zielke device. Spine 16:70–77
4. Blauth M, Knop C, Bastian L (1997) Behandlungsstrategie und Ergebnisse bei Frakturen im Bereich der BWS und LWS. Hefte Z Unfallchirurg 268:171–179
5. Blauth M, Knop C, Bastian L (1998) Brust- und Lendenwirbelsäule. In: Tscherne H, Blauth M (eds) Tscherne Unfallchirurgie – Wirbelsäule, 1st edn. Springer, Berlin Heidelberg New York, pp 241–372
6. Blauth M, Knop C, Bastian L, Lobenhoffer P (1997) Neue Entwicklungen in der Chirurgie der verletzten Wirbelsäule. Orthopade 26:437–449
7. Blauth M, Tscherne H, Gotzen L, Haas N (1987) Ergebnisse verschiedener Operationsverfahren zur Behandlung frischer Brust- und Lendenwirbelsäulenverletzungen. Unfallchirurg 90:260–273
8. Böhm H, Harms J, Donk R, Zielke K (1990) Correction and stabilization of angular kyphosis. Clin Orthop 258:56–61
9. Daniaux H, Seykora P, Genelin A, Lang T, Kathrein A (1991) Application of posterior plating and modifications in thoracolumbar spine injuries. Indication, techniques and results. Spine 16 [3 Suppl]:125-133
10. Dick W (1987) The “fixateur interne” as a versatile implant for spine surgery. Spine 12:882–900
11. Feil J, Wörsdörfer O (1992) Ventrale Stabilisierung im Bereich der Brust- und Lendenwirbelsäule. Chirurg 63: 856–865
12. Felsenberg D, Kalender WA, Banzer D, Schmilinsky G, et al (1988) Quantitative computertomographische Knochenmineralgehaltsbestimmung. Fortschr Röntgenstr 148:431–436
13. Haas N, Blauth M, Tscherne H (1991) Anterior plating in thoracolumbar spine injuries. Indication, technique, and results. Spine 16 [Suppl]:100-111
14. Hansson T, Roos B, Nachemson A (1980) The bone mineral content and ultimate compressive strength of lumbar vertebrae. Spine 5:46–55
15. Ho CP, Kim RW, Schaffler MB, Sartoris DJ (1990) Accuracy of dual-energy radiographic absorptiometry of the lumbar spine: cadaver study. Radiology 176:171–173
16. Hollowell JP, Vollmer DG, Wilson CR, Pintar FA, Yoganandan N (1996) Biomechanical analysis of thoracolumbar interbody constructs. How important is the endplate? Spine 21:1032–1036
17. Ito M, Hayashi K, Yamada M, Uetani M, Nakamura T (1993) Relationship of osteophytes to bone mineral density and spinal fracture in men. Radiology 189:497–502
18. Jost B, Cripton PA, Lund T, Oxland TR, et al (1998) Compressive strength of interbody cages in the lumbar spine: the effect of cage shape, posterior instrumentation and bone density. Eur Spine J 7:132–141
19. Kalender WA (1988) Neue Entwicklungen in der Knochendichtemessung mit quantitativer Computertomographie (QCT). Radiologe 28:173–178
20. Kaneda K, Taneichi H, Abumi K, Hashimoto T, Satoh S, Fujiya M (1997) Anterior decompression and stabilization with the Kaneda device for thoracolumbar burst fractures associated with neurological deficits. J Bone Joint Surg Am 79:69–83
21. Kluger P, Gerner HJ (1986) Das mechanische Prinzip des Fixateur externe zur dorsalen Stabilisierung der Brust- und Lendenwirbelsäule. Unfallchirurgie 12:68–79
22. Knop C, Blauth M, Bastian L, Lange U, Kesting J, Tscherne H (1997) Frakturen der thorakolumbalen Wirbelsäule – Spätergebnisse nach dorsaler Instrumentierung und ihre Konsequenzen. Unfallchirurg 100:630–639
23. Knop C, Blauth M, Bühren V, Hax P-M, et al (1999) Operative Behandlung von Verletzungen des thorakolumbalen Übergangs. 1. Epidemiologie. Unfallchirurg 102:924–935
24. Knop C, Blauth M, Bühren V, Hax P-M, et al (2000) Operative Behandlung von Verletzungen des thorakolumbalen Übergangs. 2. Operation und röntgenologische Befunde. Unfallchirurg, in press
25. Kostuik JP (1988) Anterior fixation for burst fractures of the thoracic and lumbar spine with or without neurological involvement. Spine 13:286–293
26. McBroom RJ, Hayes WC, Edwards WT, Goldberg RP, White AA, III (1985) Prediction of vertebral body compressive fracture using quantitative computed tomography. J Bone Joint Surg Am 67:1206–1214
27. Miyakoshi N, Abe E, Shimada Y, Hongo M, Chiba M, Sato K (1999) Anterior decompression with single segmental spinal interbody fusion for lumbar burst fracture. Spine 24:67–73
28. Okuyama K, Abe E, Chiba M, Ishikawa N, Sato K (1996) Outcome of anterior decompression and stabilization for thoracolumbar unstable burst fractures in the absence of neurologic deficits. Spine 21:620–625
29. Olerud S, Karlstrom G, Sjostrom L (1988) Transpedicular fixation of thoracolumbar vertebral fractures. Clin Orthop 227:44–51
30. Plaue R (1972) Das Frakturverhalten von Brust- und Lendenwirbelkoerpern. 2. Kompressionsversuche an frischen Leichenwirbeln. Z Orthop Ihre Grenzgeb 110:357–362
31. Reinbold WD, Adler CP, Kalender WA, Lente R (1991) Accuracy of vertebral mineral determination by dual-energy quantitative computed tomography. Skeletal Radiol 20:25–29
32. Resch A, Schneider B, Bernecker P, Battmann A, et al (1995) Risk of vertebral fractures in men: relationship to mineral density of the vertebral body. AJR 164:1447–1450
33. Seeger LL (1997) Bone density determination. Spine 22 [Suppl]:49-57
34. Stoltze D, Harms J (1999) Korrekturen posttraumatischer Fehlstellungen – Prinzipien und Techniken. Orthopade 28:731–745
35. von Gumppenberg S, Vieweg J, Claudi B, Harms J (1991) Die primare Versorgung der frischen Verletzungen von Brust- und Lendenwirbelsaule. Aktuelle Traumatol 21:265–273
36. Weinstein JN, McLain RF (1987) Primary tumors of the spine. Spine 12: 843–851
37. Wilke HJ, Wenger K, Claes L (1998) Testing criteria for spinal implants: recommendations for the standardization of in vitro stability testing of spinal implants. Eur Spine J 7:148–154
38. Wolfinbarger L Jr, Zhang Y, Adam BL, Sutherland V, Gates K, Brame B (1994) A comprehensive study of physical parameters, biomechanical properties, and statistical correlations of iliac crest bone wedges used in spinal fusion surgery. II. Mechanical properties and correlation with physical parameters. Spine 19:284–295
39. Yuan HA, Mann KA, Found EM, Helbig TE, et al (1988) Early clinical experience with the Syracuse I-plate: an anterior spinal fixation device. Spine 13:278–285
40. Zangger P, Pache T (1993) Reduction and stabilization of lumbar and thoracolumbar spine fractures with Louis’ plates and internal fixator: a comparative study. Eur Spine J 2:159–164